Available online at www.sciencedirect.com
SCIENCE DIRECT®
Thermochimica Acta 414 (2004) 227–232
thermochimica acta
www.elsevier.com/locate/tca

The effect of chromium substitution on the phase transition of lithium manganese spinel oxides

Hiromasa Ikuta, Kouichi Takanaka, Masataka Wakihara*

Department of Applied Chemistry, Tokyo Institute of Technology, 2-12-1 Ookayama, Meguro-ku, Tokyo 152-8552, Japan

Received 27 June 2003; received in revised form 25 December 2003; accepted 7 January 2004

Abstract

The phase transition of chromium substituted lithium manganese spinel oxide, $LiCr_yMn_{2-y}O_4$ was investigated by low-temperature powder X-ray diffractometry (XRD), differential scanning calorimetry (DSC), and electrical resistivity measurements. The sample prepared at 820 °C resulted in lowering the transition temperature T_t with Cr composition y, whereas T_t of the sample prepared at 750 °C remained constant for $0 \leq y \leq 0.17$ in $LiCr_yMn_{2-y}O_4$. This would be caused by a difference in distribution of the substituted Cr^{3+} ion in octahedral site depending on the preparation temperature. The phase transition was suppressed with increasing the amount of Cr content.

Keywords: Lithium manganese spinel oxide; $LiMn_2O_4$; Cooperative Jahn–Teller distortion; Phase transition; Chromium substitution

1. Introduction

Lithium manganese spinel oxide $LiMn_2O_4$ has been intensively investigated as one of the most promising cathode material for large-scale lithium rechargeable battery [1–6] because of rich abundance of manganese resources, low-toxicity of manganese ion and high decomposition temperature at fully charged state compared with $LiCoO_2$ or $LiNiO_2$ cathodes. $LiMn_2O_4$ has a cubic normal spinel structure and belongs to the space group $Fd\bar{3}m$. When reversible delithiation from $LiMn_2O_4$ occurs electrochemically at around 4 V versus Li/Li^+, the Li^+ ion intercalated in or deintercalated from cubic single phase ($0.5 < x < 1$) or cubic–cubic two phases ($0 < x < 0.5$) in $Li_xMn_2O_4$. Slow capacity fading was encountered in this 4 V region for stoichiometric $LiMn_2O_4$ cathode. Among a great number of investigations trying to improve the cycling efficiency, some groups [3–6] have reported that $LiMn_2O_4$ in which manganese ions were partially substituted by other mono-, di-, or tri-valent cations offered better electrochemical stability. All the results are naturally associated with the increase of the average oxidation state of manganese, which leads to the decrease of Mn^{3+}. In general, $LiM_yMn_{2-y}O_4$ has offered better cycleability without remarkable capacity fading of the parent $LiMn_2O_4$ if the composition of the substituted metal y is less than 1/3. Therefore, $LiM_yMn_{2-y}O_4$ is one of the most promising cathode materials for rechargeable lithium batteries.

On the other hand, several research groups have focused on the structural and physical properties of $LiMn_2O_4$ because of its phase transition occurring around room temperature. Yamada and Tanaka [7] firstly reported that the stoichiometric $LiMn_2O_4$ undergoes a structural phase transition at about 280 K from high-temperature cubic ($Fd\bar{3}m$) phase to low-temperature tetragonal ($I4_1/amd$) phase due to the Jahn–Teller distortion in the $Mn^{3+}O_6$ octahedra on the analogy of electrochemically prepared $Li_2Mn_2O_4$. They have thought that the tetragonal phase coexisted with cubic phase even at low-temperature. On the other hand, Oikawa et al. [8] have reported that the transition occurred from cubic at high-temperature to orthorhombic ($Fddd$) at low-temperature. They also have pointed out the existence of superlattice peaks caused by a superstructure. Rodriguez-Carvajal and coworkers [9,10] have reveled that low-temperature orthorhombic phase has $3 \times 3 \times 1$ superstructure, which is caused by a charge ordering of manganese ion in the system, namely ordering of distribution of Mn^{3+} and Mn^{4+} occurred. In recent years, Takada

* Corresponding author. Tel.: +81-3-5734-2145; fax: +81-3-5734-2146.
E-mail address: mwakihar@o.cc.titech.ac.jp (M. Wakihara).

0040-6031/$ – see front matter © 2004 Elsevier B.V. All rights reserved.
doi:10.1016/j.tca.2004.01.009

and coworkers [11,12] have reported that the orthorhombic phase further transforms to tetragonal ($I4_1/amd$) phase at around 65 K. Wills et al. [13] have detected the antiferromagnetic transition at around 65 K by neutron diffraction, and they concluded that the antiferromagnetic transition originates the formation of long-range ordering of manganese ions, i.e. Mn^{3+} and Mn^{4+}.

On the effect of other metal substitution in manganese site to the phase transition at room temperature, Yamada et al. [14] have reported that the transition is suppressed by the increase of Li in $Li_{1+y}Mn_{2-y}O_4$. In the same way, the substitution by Mg [15] or Co [16] also suppressed the phase transition.

In the present study, we investigated the effect of Cr substitution on a structural phase transition of $LiMn_2O_4$ due to the Jahn–Teller distortion by differential scanning calorimetry (DSC), low-temperature X-ray diffractometry (XRD) and by electrical resistivity measurements. We found that the phase transition temperature depends not only on the Cr composition but also on the preparation temperature of the sample from the DSC analysis.

2. Experimental

Polycrystalline $LiCr_yMn_{2-y}O_4$ samples with Cr range $0 \leq y \leq 1.0$ were prepared by reacting an appropriate amount of mixture of Mn_2O_3, Li_2CO_3 (99.9%, Soekawa Chemical Co., Ltd.), and Cr_2O_3 (99.9%, Soekawa Chemical Co., Ltd.) at 750–820 °C for 72 h in air, followed by quenching. Mn_2O_3 was preliminarily obtained by decomposing $MnCO_3$ (99.9%, Soekawa Chemical Co., Ltd.) at 600 °C for 48 h in air.

Powder X-ray diffraction of the samples was carried out using Cu Kα radiation equipped with a curved graphite monochromator (Rigaku RINT 2500 V). Low-temperature powder X-ray diffraction data were collected at several constant temperatures during cooling down from 298 to 223 K.

DSC analysis of the prepared samples (about 0.020 g) was performed with a Shinku-Riko DSC 9100 thermal analyzer in dry air at 9.7×10^4 Pa between 213 and 323 K. α-Al_2O_3 was used as a reference material. The scan rate was controlled about 5 K min^{-1} on heating.

For dc resistivity measurement, the prepared sample of about 0.3 g was uniaxially pressed into a cylindrical pellet at 2.0×10^6 Pa, and then sintered at 820 °C for 96 h. The dimension of the pellet was 5 mm in diameter and 5 mm in length. The dc resistivity measurements were made by using four-probe method at a current of 1 μA between 220 and 320 K for the samples $LiCr_yMn_{2-y}O_4$ except for $LiCrMnO_4$. The dc measurement for the sample $LiCrMnO_4$ was carried out between 310 and 355 K because of its higher resistivity compared with the other samples. The cooling or heating rate was controlled at 1 K min^{-1}.

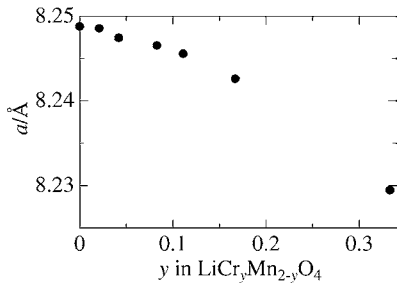

Fig. 1. Cubic lattice parameters a for $LiCr_yMn_{2-y}O_4$ with y prepared at 820 °C.

3. Results and discussion

3.1. Structural phase transition

All the prepared samples, $LiCr_yMn_{2-y}O_4$ with a composition range $0 \leq y \leq 1.0$ were identified as a single phase with a cubic spinel ($Fd\bar{3}m$) from the X-ray diffraction patterns. No peaks corresponding to impurity phases such as Cr_2O_3 could be observed in the patterns. In Fig. 1, the cubic lattice parameters a are plotted against chromium composition y in $LiCr_yMn_{2-y}O_4$. The lattice parameter a decreased with increasing y, because ionic size of substituted Cr^{3+} is smaller than that of Mn^{3+} as described in our previous paper [6].

The DSC curve of the $LiMn_2O_4$ prepared at 820 °C is shown in Fig. 2. The reversible phase transition occurred in the sample accompanied a temperature hysteresis of about 20 K. Fig. 3a and b show the variation of DSC peaks of $LiCr_yMn_{2-y}O_4$ depending on the Cr composition prepared at 820 and 750 °C, respectively. By comparing the curves in Fig. 3a with those in Fig. 3b, it is found that the T_t of the samples prepared at 820 °C shifted to lower temperature with the increase of Cr ratio. Wojtowicz [17] has discussed the Jahn–Teller phase transition from tetragonal to cubic symmetry using theoretical statistical model. He has explained the phase transition using a cooperative interaction among nearest neighboring Jahn–Teller ions. If the spinel oxide has the formula $AB_{2-2x}C_{2x}O_4$ in which the non-Jahn–Teller C ions randomly replace the Jahn–Teller B ions in the octahedral 16d sites, the transition temperature $T_t(x)$ depending on the composition x of the non-Jahn–Teller ions can be described as follows:

$$T_t(x) = (1 - x)T_t(0)$$

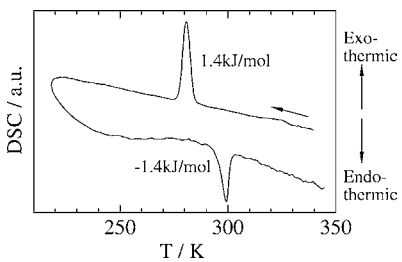

Fig. 2. DSC cooling curves for $LiMn_2O_4$ prepared at 820 °C.

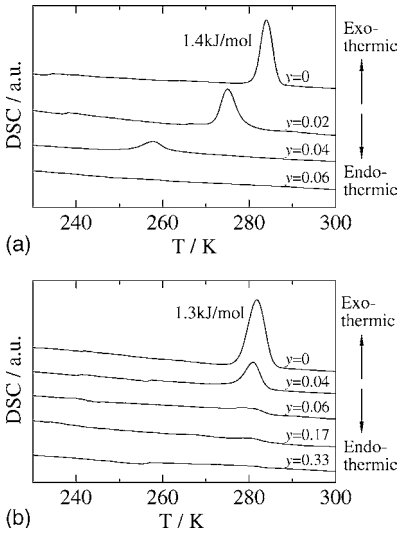

Fig. 3. (a) DSC cooling curves for $LiCr_yMn_{2-y}O_4$ with y prepared at 820 °C. (b) DSC cooling curves for $LiCr_yMn_{2-y}O_4$ with y prepared at 750 °C.

where $T_t(0)$ is the transition temperature of the parent material filled with the Jahn–Teller ions in the 16*d* sites. In this model, the Jahn–Teller ions distribute randomly with the non-Jahn–Teller ions. This equation shows that the degree of lowering of the transition temperature is proportional to the fraction of the non-Jahn–Teller ions. According to the Wojtowicz theorem, the transition temperature should decrease with the increase of substitution amount of the non-distorted ions (Cr^{3+}) for the distorted ions (Mn^{3+}), and the results of DSC analysis completely obeyed his theorem for the samples prepared at 820 °C. A latent heat corresponding to the transition also decreased with the increase of Cr composition as shown in Fig. 3a, and the variation depending on y values is shown in Fig. 4. On the other hand, the T_t of the sample prepared at 750 °C remained constant for $0 \leq y \leq 0.17$ in $LiCr_yMn_{2-y}O_4$ as shown in Fig. 3b. This result does not obey the Wojtowicz theorem. As described above, no second phase was observed for all the prepared samples. The distribution of the Cr^{3+} ion in the octahedral site might not be inhomogeneous for the sample prepared at relatively low-temperature such as 750 °C. These results will be discussed minutely at the following section.

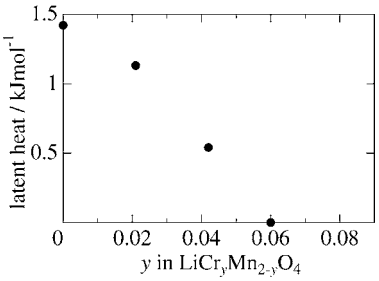

Fig. 4. Latent heats estimated from DSC curves for $LiCr_yMn_{2-y}O_4$ with y prepared at 820 °C.

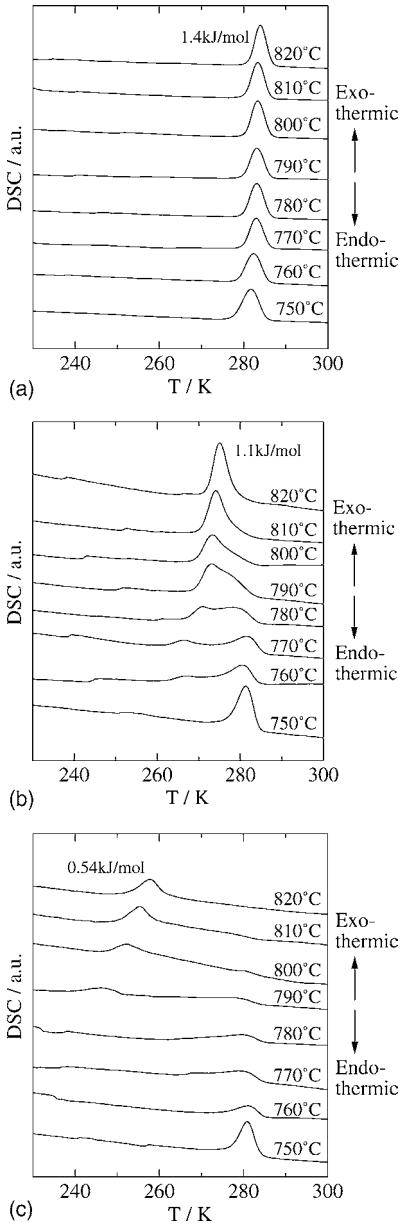

Fig. 5. (a) DSC cooling curves for $LiMn_2O_4$ prepared at various temperatures. (b) DSC cooling curves for $LiCr_{0.02}Mn_{1.98}O_4$ prepared at various temperatures. (c) DSC cooling curves for $LiCr_{0.04}Mn_{1.96}O_4$ prepared at various temperatures.

Fig. 5a–c show DSC curves at various preparation temperatures for $LiMn_2O_4$, $LiCr_{0.02}Mn_{1.98}O_4$, and $LiCr_{0.04}Mn_{1.96}O_4$, respectively. In the case of $LiMn_2O_4$, there were no differences in the T_t values of DSC curves with the change of calcination temperature as shown in Fig. 5a. On the contrary, two exothermic peaks on cooling process were observed for $LiCr_{0.02}Mn_{1.98}O_4$ prepared between 760 and 810 °C (Fig. 5b). The area of the peaks appeared at around 280 K decreased with the increase of preparation temperature, and that appeared below 280 K increased. The former peak could not be observed in $LiCr_{0.02}Mn_{1.98}O_4$ prepared at 820 °C. Moreover, the latter

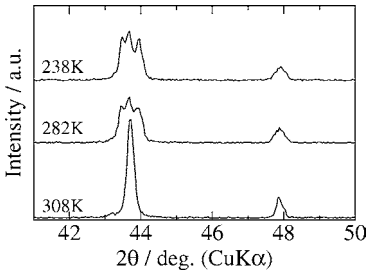

Fig. 6. Low-temperature XRD patters for $LiMn_2O_4$ prepared at 820 °C.

peak was remarkably shifted to higher temperature with increasing preparation temperature. The similar peaks were observed for the $LiCr_{0.04}Mn_{1.96}O_4$, and the differences of the two peak-temperatures were larger than those for the $LiCr_{0.02}Mn_{1.98}O_4$ as shown in Fig. 5c.

Fig. 6 shows the low-temperature XRD pattern of $LiMn_2O_4$ prepared at 820 °C. At 282 K, the (4 0 0) peak at around $2\theta = 44^\circ$ of the cubic $LiMn_2O_4$ phase split into three peaks corresponding to orthorhombic phase [8]. The splitting was observed more clearly at 238 K. The difference between the splits observed at 238 and 282 K should be related to the long-range ordering of the orientation of the distorted octahedron. The XRD pattern with the only one exothermic peak observed in DSC analysis on cooling process (Fig. 5) for $LiCr_{0.04}Mn_{1.96}O_4$ prepared at 750 °C and that with two exothermic peaks observed analysis on cooling process prepared at 790 °C are presented in Fig. 7a and b, respectively. XRD measurements were carried out at several points around transition temperature. There is no apparent change on the shape of the diffraction peak between 223 and 258 K for the sample prepared at 750 °C. On the other hand, it is observed that the split of diffraction

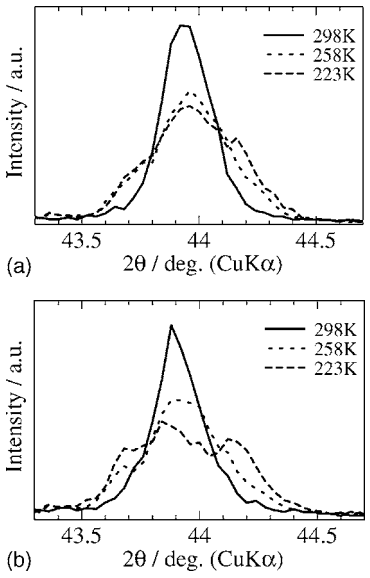

Fig. 7. (a) Low-temperature XRD patters for $LiCr_{0.04}Mn_{1.96}O_4$ prepared at 750 °C. (b) Low-temperature XRD patters for $LiCr_{0.04}Mn_{1.96}O_4$ prepared at 790 °C.

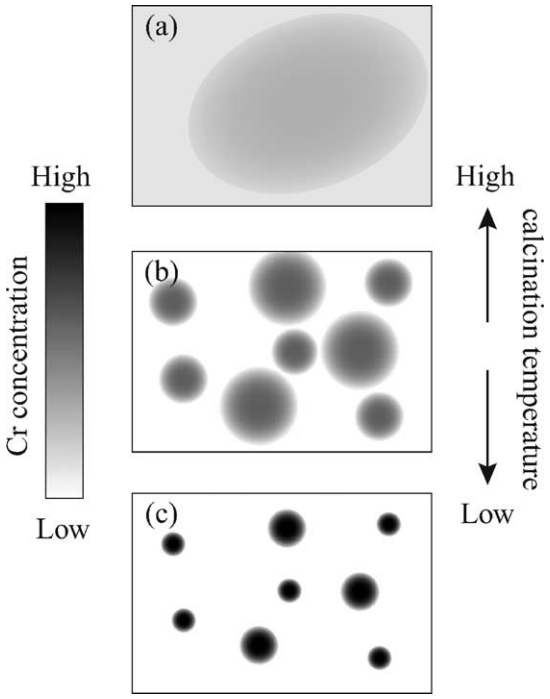

Fig. 8. Schematic figures of the distribution of Cr ion in the spinel oxides prepared at (a) high, (b) middle, and (c) low-temperature.

peak measured at 223 K for the sample prepared at 790 °C is much more clearer than the one measured at 258 K.

From the DSC and the XRD measurements, we schematically illustrate Cr distribution in the sample at different calcination temperature in Fig. 8a–c. The Cr distribution in the sample prepared at relatively high-temperature would be homogeneous as shown in Fig. 8a. On the contrary, the Cr distribution in the sample prepared at relatively low-temperature would be inhomogeneous as presented in Fig. 8c. The phase transition was suppressed in the region of high Cr concentration. It was observed that the phase transition was much more clearly in the low Cr concentration region in which the composition is nearly "$LiMn_2O_4$." In the sample prepared at intermediate temperature, two exothermic peaks were observed on cooling process on DSC analysis (Fig. 8b). The phase transition for the Cr substituted spinels prepared at intermediate temperature would be induced at around 280 K in the low Cr concentration region at first. After that the second phase transition would occur at around 245 K in the high Cr concentration region as observed in Fig. 5c.

Recently, Kanno et al. [18] have reported that the phase transition temperature is affected by the non-stoichiometry of oxygen in the spinel sample prepared by changing synthesis temperature and atmosphere. They have concluded that the oxygen vacancy exists in the sample synthesized above 800 °C. Kanno et al. [19] have already reported that the cubic manganese spinel has oxygen vacancy at 32*e* site with interstitial oxygen at 8*b* site in the sample prepared at 900 °C by the precise structure analysis using

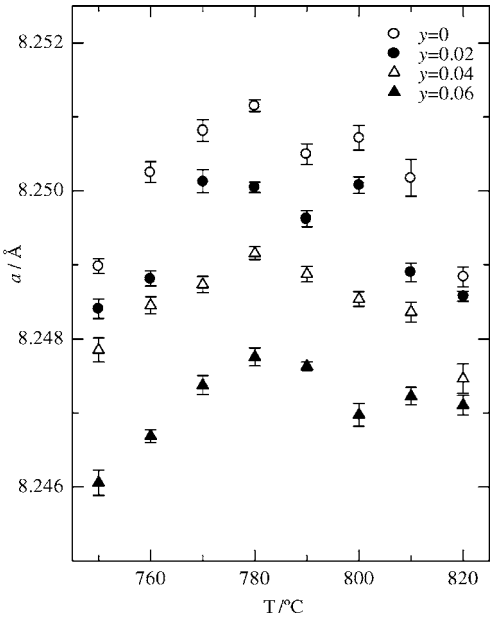

Fig. 9. Cubic lattice parameters a depending on preparation temperature for $LiCr_yMn_{2-y}O_4$.

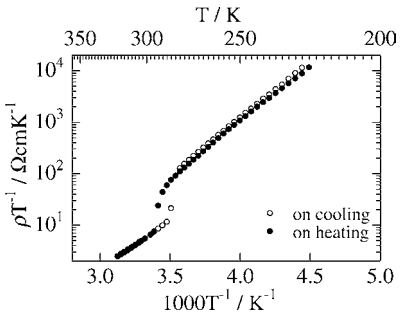

Fig. 10. Arrhenius plots ρ/T for $LiMn_2O_4$.

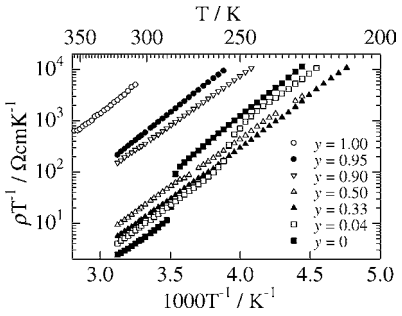

Fig. 11. Arrhenius plots ρ/T for $LiCr_yMn_{2-y}O_4$.

neutron diffraction. Against their results, our research group [20,21] has proposed the cation excess model to explain the non-stoichiometry of the lithium manganese spinel oxides detected by density measurement. As shown in our previous paper [21], the lattice parameter of the non-stoichiometric spinel oxides increases with increasing non-stoichiometry. In this experiments, the lattice parameter with preparation temperature changed as shown in Fig. 9. All the samples were prepared under air atmosphere in the present study. The lattice parameter decreases with increasing substituted Cr composition on isothermal condition as already shown in Fig. 1, however, convex curves are obtained for all the prepared Cr composition range on the preparation temperature. The lattice parameter increased with increasing preparation temperature up to 790 °C. This tendency would be caused by the reduction of manganese ions in the homogeneous region. Contrary to this tendency, the lattice parameter decreased with increasing preparation temperature above 790 °C. The distribution of transition metal ions prepared at high-temperature should become more homogeneous than the sample at low-temperature. This change in ionic distribution would affect the decrease of the lattice parameter. Considering unchanged width of the diffraction peak for all the prepared samples, the degree of inhomogeneity would not be detected by an ordinal X-ray diffraction technique. Accordingly, the degree of local ionic distribution is an important factor to the transition of lithium manganese spinel oxides. In order to make sure whether this hypothesis is true or not, we are currently investigating the local structure of the lithium manganese spinel oxides using molecular dynamics simulation and spectroscopic measurements.

3.2. Effect of phase transition on the electrical resistivity

The anomaly with some hysteresis was observed on conductivity for $LiMn_2O_4$ as shown in Fig. 10. This behavior reflects the hysteresis of the phase transition and it was in good agreement with the result reported by Shimakawa et al. [22]. For $LiCr_yMn_{2-y}O_4$, the anomaly was observed for each $LiCr_yMn_{2-y}O_4$ sample at $0 \leq y \leq 0.04$ (Fig. 11), in which the existence of the phase transition was already confirmed by DSC as shown above section. The activation energy E_a in the equation of $\rho/T = \rho_0 \exp(-E_a/kT)$ was evaluated to be 0.43 and 0.35 eV below and above T_t, respectively. In $LiMn_2O_4$, Sugiyama et al. [23] and Massarotti et al. [24] have already reported that the small polaron is a carrier. The resistivity at 310 K and activation energy estimated above T_t with y in $LiCr_yMn_{2-y}O_4$ are shown in Fig. 12. It was found that the resistivity rapidly increased in the $LiCr_yMn_{2-y}O_4$ sample near $y = 1.0$. This phenomenon could be induced by the extremely small amount of Mn^{3+} which makes a role of

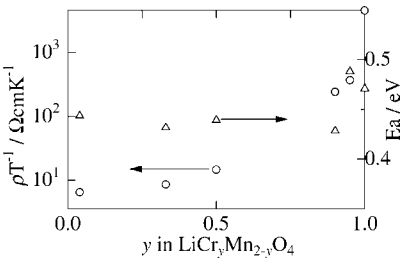

Fig. 12. Cr composition dependence of ρ/T at 310 K and activation energy.

a carrier of charge transfer for small polarons hopping with Mn^{4+}. The activation energy is almost constant at around 0.43 eV up to $y = 0.9$, however, suddenly rises to larger than 0.48 eV above $y = 0.95$. Sugiyama et al. [23] and Massarotti et al. [24] have reported that the activation energy of the resistivity is estimated to be 0.39 and 0.4 eV for $LiMn_2O_4$, respectively. Moreover, Atanasov et al. [25] have reported that the activation energy is estimated to be 0.445 eV based on the calculation by density function theory. According to previous reports, our estimated activation energy 0.43 eV would be reasonable value for $LiCr_yMn_{2-y}O_4$ system oxides by small polaron model in Mn^{3+}–Mn^{4+} mixed-valent mechanism. On the other hand, the activation energy values higher than 0.48 eV observed in the present sample near $y = 1$ is slightly higher value for Mn^{3+}–Mn^{4+} mixed-valent mechanism. This activation energy value may be associated with other mechanisms such as Mn^{4+}–Cr^{3+} or Cr^{3+}–Cr^{4+}. For example, Moriwake et al. [26] have reported the activation energy value 0.55 eV of resistivity for $MgCr_2O_4$ with normal spinel structure. The participation of Cr ions would induce the sudden increase of the activation energy.

4. Conclusions

In this study, we demonstrated that partial substitution of chromium for manganese on the octahedral sites led to the suppression of the cooperative Jahn–Teller distortion of $LiMn_2O_4$. The results of the DSC and the low-temperature XRD measurements indicate that the effect of substitution largely depends on the preparation temperature. Partial substitution of Cr^{3+} for Mn^{3+} results in the modification of the transport property of $LiMn_2O_4$ as a semiconductor remains over the range $0 \leq y \leq 1.0$ in $LiCr_yMn_{2-y}O_4$.

Acknowledgements

This work was supported by Grant-in-Aid for Scientific Research on Priority Areas (B) (No. 740) “Fundamental Studies for Fabrication of All Solid State Ionic Devices” from Ministry of Education, Culture, Sports, Science and Technology.

References

[1] M.M. Thackeray, P.J. Johnson, L.A. de Picciotto, P.G. Bruce, J.B. Goodenough, Mater. Res. Bull. 19 (1984) 179.
[2] T. Ohzuku, M. Kitagawa, T. Hirai, J. Electrochem. Soc. 137 (1990) 769.
[3] J.M. Tarascon, E. Wang, F.K. Shokoohi, W.R. McKinnon, S. Colson, J. Electrochem. Soc. 138 (1991) 2859.
[4] G. Pistoia, G. Wang, Solid State Ionics 66 (1993) 135.
[5] R.J. Gummow, A. de Kock, M.M. Thackeray, Solid State Ionics 69 (1994) 58.
[6] Li Guohua, H. Ikuta, T. Uchida, M. Wakihara, J. Electrochem. Soc. 143 (1996) 178.
[7] A. Yamada, M. Tanaka, Mater. Res. Bull. 30 (1995) 715.
[8] K. Oikawa, T. Kamiyama, F. Izumi, B.C. Chakoumakos, H. Ikuta, M. Wakihara, Y. Matsui, Solid State Ionics 109 (1998) 35.
[9] J. Rodriguez-Carvajal, G. Rousse, C. Masquelier, M. Hervieu, Phys. Rev. Lett. 81 (1998) 21.
[10] G. Rousse, C. Masquelier, J. Rodriguez-Carvajal, M. Hervieu, Electrochem. Solid State Lett. 2 (1999) 6.
[11] H. Hayakawa, T. Takada, H. Enoki, E. Akiba, J. Mater. Sci. Lett. 17 (1998) 811.
[12] T. Takada, H. Hayakawa, H. Enoki, E. Akiba, H. Slegr, I. Davodson, H. Murray, J. Power Sources 81 (1999) 505.
[13] A.S. Wills, N.P. Raju, J.E. Greendan, Chem. Mater. 11 (1999) 1510.
[14] A. Yamada, K. Miura, K. Hinokuma, M. Tanaka, J. Electrochem. Soc. 142 (1995) 2149.
[15] R. Basu, R. Seshadri, J. Mater. Chem. 10 (2000) 507.
[16] C.-H. Shen, R. Gundakaram, R.-S. Liu, H.-S. Sheu, J. Chem. Soc., Dalton Trans. 37 (2001) 37.
[17] P.J. Wojtowicz, Phys. Rev. 116 (1959) 32.
[18] R. Kanno, M. Yonemura, T. Kohigashi, Y. Kawamoto, M. Tabuchi, T. Kamiyama, J. Power Sources 97–98 (2001) 423.
[19] R. Kanno, A. Kondo, M. Yonemura, R. Gover, Y. Kawamoto, M. Tabuchi, T. Kamiyama, F. Izumi, C. Masquelier, G. Rousse, J. Power Sources 81 (1999) 542.
[20] M. Hosoya, H. Ikuta, T. Uchida, M. Wakihara, J. Electrochem. Soc. 144 (1997) L52.
[21] M. Hosoya, H. Ikuta, M. Wakihara, Solid State Ionics 111 (1998) 153.
[22] Y. Shimakawa, T. Numata, J. Tabuchi, J. Solid State Chem. 131 (1997) 138.
[23] J. Sugiyama, T. Atsumi, K. Koiwa, T. Sasaki, T. Hioki, S. Noda, N. Kamegashira, J. Phys. Condensed Mater. 9 (1997) 1729.
[24] V. Massarotti, D. Capsoni, M. Bini, G. Chiodelli, C.B. Azzoni, M.C. Mozzati, A. Paleari, Solid State Ionics 131 (1997) 94.
[25] M. Atanasov, J.-L. Barras, L. Benco, C. Daul, J. Am. Chem. Soc. 122 (2000) 4718.
[26] H. Moriwake, T. Hata, M. Katsumata, M. Takahashi, I. Shimono, J. Ceram. Soc. Jpn. 107 (1999) 258.